Isolation of Bioactive Compounds from *Melastoma Malabathricum* (Keduruk) for Antibacterial Activity Against *Staphylococcus aureus* and *Pseudomonas aeruginosa* to Promote Wound Healing

Harizon [a,1], Febbry Romundza [a,2,*], Harlis [a,3], Mia Aina [a,4], Asmiyunda [a,5]

[a] Department of Chemistry Education, Faculty of Teacher Training and Education, Universitas Jambi, Jambi, Indonesia
[1] harizon@unja.ac.id; [2] febbryromundza@unja.ac.id*; [3] harlis@unja.ac.id; [4] miaaina@unja.ac.id; [5] asmiyunda@unja.ac.id
* corresponding author

ARTICLE INFO

Article history
Received September 9, 2025
Revised September 16, 2025
Accepted September 20, 2025

Keywords
Melastoma malabathricum
Bioactive compounds
Antibacterial
Wound healing
Topical formulation

ABSTRACT

Melastoma malabathricum (keduruk) is a traditional medicinal plant widely used in Southeast Asia for wound healing. However, studies on its bioactive compounds and antibacterial activity remain limited. This study aimed to isolate and identify antibacterial compounds from M. malabathricum leaves and evaluate their potential for topical wound-healing applications. Fresh leaves were extracted using 70% ethanol via maceration, followed by liquid–liquid partitioning and chromatographic purification. Phytochemical screening confirmed the presence of flavonoids, tannins, saponins, alkaloids, and terpenoids. Among the fractions, the ethyl acetate extract exhibited the strongest antibacterial activity and was subjected to further isolation and characterization using ^{1}H-NMR, ^{13}C-NMR, and HR-TOF-MS, revealing flavonoid derivatives as the major constituents. Antibacterial activity was tested by the disk diffusion method against Staphylococcus aureus ATCC 25923 and Pseudomonas aeruginosa ATCC 27853. At 10,000 µg/mL, the ethanol extract produced inhibition zones of 15.6 ± 0.6 mm against S. aureus and 12.1 ± 0.5 mm against P. aeruginosa. The isolated flavonoid compound showed stronger inhibition—19.2 ± 0.6 mm and 16.7 ± 0.5 mm, respectively—comparable to gentamicin (22.8 ± 0.7 mm and 21.5 ± 0.6 mm). The antibacterial effect was more pronounced against Gram-positive bacteria, likely due to structural differences in the cell wall. Overall, M. malabathricum leaves, particularly the ethyl acetate fraction and its flavonoid constituents, demonstrate strong antibacterial potential and could serve as natural candidates for developing topical formulations to support wound healing.

1. Introduction

Wound healing is a complex and organized biological process that involves several physiological stages, including hemostasis, inflammation, proliferation, and tissue remodeling. The primary goal of this process is to restore the structure and function of tissue damaged by trauma or injury [1]. However, the success of wound healing is often hindered by bacterial infections, which can prolong the inflammatory phase and disrupt normal tissue regeneration [2]. Two of the most common pathogenic bacteria found in infected wounds are *Staphylococcus aureus* and *Pseudomonas aeruginosa*. These microorganisms are capable of forming biofilms and exhibiting resistance to various conventional antibiotics, which delays the healing process and increases the risk of complications such as abscesses, tissue necrosis, and even sepsis [3]. Furthermore, the widespread and irrational use of synthetic antibiotics has contributed to the alarming rise in global antimicrobial resistance, which presents a serious challenge in modern medical treatment [4].

In response to these issues, the utilization of natural products as alternative sources of antimicrobial and wound-healing agents has gained increasing relevance. Medicinal plants are known to contain a wide range of secondary metabolites that exhibit antibacterial, anti-inflammatory, and antioxidant properties [5]. One such promising plant is *Melastoma malabathricum*, locally known as "keduruk." This plant has been traditionally used to treat wounds, mouth ulcers, and skin infections [6]. Preliminary studies have reported that the leaves of *M. malabathricum* are rich in flavonoids, tannins, and saponins—compounds known to inhibit bacterial growth and promote tissue regeneration by modulating the inflammatory response [7]. Despite the promising potential of *M. malabathricum*, systematic scientific studies focusing on the isolation of active compounds, antibacterial efficacy against wound-infecting pathogens, and the development of practical topical formulations are still limited [8]. In fact, the formulation of topical preparations such as gels or ointments is crucial to ensure compound stability, effective delivery of active ingredients to the wound site, and ease of application [9].

Based on the considerations mentioned above, this study aims to achieve three main objectives: (1) to isolate and identify bioactive compounds from *Melastoma malabathricum* leaves; (2) to evaluate their antibacterial activity against *Staphylococcus aureus* and *Pseudomonas aeruginosa*; and (3) to develop a safe and effective gel-based topical formulation to enhance wound healing. This research is expected to contribute to the development of evidence-based natural therapeutics for managing infected wounds [10].

2. Research Methodology

2.1. Plant Material Collection and Extraction

Fresh leaves of *Melastoma malabathricum* were collected from the Bukit Dua Belas forest area in Jambi Province, Indonesia. The plant was authenticated at the Herbarium of Universitas Jambi. The leaves were washed, air-dried at room temperature, and ground into fine powder. Extraction was carried out using 70% ethanol maceration with a 1:10 w/v ratio (500 g of leaf powder to 5,000 mL of solvent) for 3 × 24 hours. The extract was concentrated under vacuum at 40 °C and subsequently partitioned successively with *n*-hexane and ethyl acetate. Purification was performed using a silica gel 60 column (230–400 mesh; column dimensions: 60 × 3 cm) with a gradient elution program of *n*-hexane → ethyl acetate → methanol. The flow rate was approximately 5 mL/min, and fractions were collected every 10–15 mL and combined based on their TLC profiles. The disk diffusion assay was conducted using 20 µL of sample solution impregnated onto each disk. To deliver 200 µg/disk, a sample solution concentration of 10,000 µg/mL (10 mg/mL) was used. The minimum inhibitory concentration (MIC) and minimum bactericidal concentration (MBC) were determined using the microdilution method, as outlined in CLSI guidelines, with concentration ranges adjusted accordingly for the extract, fractions, and isolated compounds.

2.2. Phytochemical Screening

Preliminary phytochemical screening of the ethanol extract was conducted to detect the presence of primary and secondary metabolites, including flavonoids, tannins, saponins, alkaloids, and terpenoids, using standard qualitative methods [11].

2.3. Isolation and Characterization of Bioactive Compounds

Purification of the active fraction was performed using column chromatography with silica gel 60 (230–400 mesh). For the preparative scale (column Ø5 cm × silica height ≈30 cm; Vcol ≈589 mL), the column was operated at a flow rate of ≈12 mL·min^{-1} with a stepwise gradient elution program of n-hexane → ethyl acetate as follows: 100:0 (1 Vcol), 90:10 (1 Vcol), 80:20 (1 Vcol), 70:30 (1 Vcol), 60:40 (1 Vcol), 50:50 (1 Vcol), 30:70 (1 Vcol), and 0:100 (1 Vcol), followed if necessary by EtOAc:MeOH (95:5 → 90:10 → 0:100; 0.5 Vcol each step). Fractions were collected every 25–30 mL and monitored by TLC (eluent system n-hexane:EtOAc 7:3; visualization under UV 254/366 nm and vanillin–H_2SO_4). Fractions showing identical TLC profiles were pooled, and each pool was concentrated under vacuum (≤40 °C) for antibacterial activity testing and further purification. For rapid purification or when using an automated system, flash chromatography can be applied using a gradient of % EtOAc in n-hexane based on Vcol (e.g., ramping 0→100% EtOAc within several Vcol), with a flow rate of 30–60 mL·min^{-1} and fraction collection of 10–30 mL; monitoring and pooling were carried out in the same manner.

The crude extract was subjected to liquid-liquid partitioning followed by chromatographic separation using column chromatography with a gradient elution method (n-hexane, ethyl acetate, and methanol). Fractions were monitored using thin-layer chromatography (TLC). The most active fraction (based on antibacterial screening) was further purified, and the isolated compounds were structurally characterized using ^{1}H-NMR, ^{13}C-NMR, and high-resolution TOF-MS spectroscopy [12].

2.4. Bacterial Strains and Culture Conditions

Two pathogenic bacterial strains were used: *Staphylococcus aureus* (ATCC 25923) and *Pseudomonas aeruginosa* (ATCC 27853). The strains were obtained from the Microbiology Laboratory at the Faculty of Medicine, Universitas Jambi. Bacteria were cultured on Nutrient Agar and maintained at 37°C before use. Nevertheless, further studies are required to determine MIC and MBC values, evaluate antibiofilm activity, and conduct in vivo testing on infected wound models to ensure both therapeutic efficacy and safety.

1) *Brief procedure (broth microdilution, CLSI/EUCAST standard)*
   a) *Medium: Mueller–Hinton Broth (MHB) for non-fastidious bacteria.*
   b) *Inoculum: Adjust to 0.5 McFarland, then dilute to ~5 × 10^5 CFU/mL in each well of a 96-well plate.*
   c) *Incubation: 35 ± 2 °C for 16–20 h with the microplate covered.*
   d) *Solvent: Use minimal DMSO/EtOH; ensure the final solvent concentration is ≤1% v/v in each well (include solvent control).*
   e) *MIC determination: Record as "no visible turbidity" by eye; optionally, resazurin/AlamarBlue can be added to enhance contrast in viability changes.*
   f) *MBC determination: From wells at or above the MIC, spot 10 µL onto compound-free MHA; incubate for 24 h. MBC is the lowest concentration that reduces viability by ≥99.9% (no colony growth).*
   g) *Quality/standard references: Follow general criteria from CLSI M07/M100 and EUCAST for inoculum preparation, medium selection, and reading endpoints.*
2) *Concentration design (two-fold serial dilutions; adjust as needed)*
   a) *Crude extract: 0.031–32 mg/mL (or a range that covers observable effects).*
   b) *Active ethyl acetate fraction: 0.016–16 mg/mL.*
   c) *Pure isolate (flavonoid): 0.002–2 mg/mL (starting lower due to typically higher potency).*
   d) *Controls: medium only, inoculum only, solvent control (≤1%), and positive control with gentamicin as an internal reference*

2.5. Antibacterial Activity Assay

Antibacterial activity was evaluated using the disk diffusion method on Mueller-Hinton Agar (MHA) with sterile paper disks (6 mm in diameter) impregnated with 20 µL of the sample solution. The 70% ethanol extract was tested at a concentration of 500 µg/µL, corresponding to 10,000 µg/disk; the ethyl acetate fraction at 250 µg/µL (5,000 µg/disk); and the purified flavonoid isolate at 100 µg/µL (2,000 µg/disk). Gentamicin (10 µg/disk) was used as the positive control, while DMSO served as the negative control. Following incubation at 37 °C for 18–24 hours, the diameter of the inhibition zones was measured in millimeters. Antibacterial activity of the ethanol extract and isolated compounds was evaluated using the disc diffusion method. Mueller-Hinton Agar (MHA) plates were inoculated with bacterial suspensions (0.5 McFarland standard). Sterile paper discs (6 mm) were impregnated with 20 µL. Gentamicin (10 µg) was used as a positive control, and DMSO as a negative control. Plates were incubated at 37°C for 24 hours, and the diameter of inhibition zones was measured in millimeters.

3. Results and Discussion

Extraction of *Melastoma malabathricum* leaves with 70% ethanol successfully yielded a crude extract rich in both polar and semi-polar secondary metabolites as shown in Fig. 1.. The selection of 70% ethanol as the solvent was based on its ability to extract both polar compounds (flavonoids, tannins, and saponins) and semi-polar compounds (alkaloids and terpenoids), which are known to play essential roles in antibacterial activity and wound healing [13].

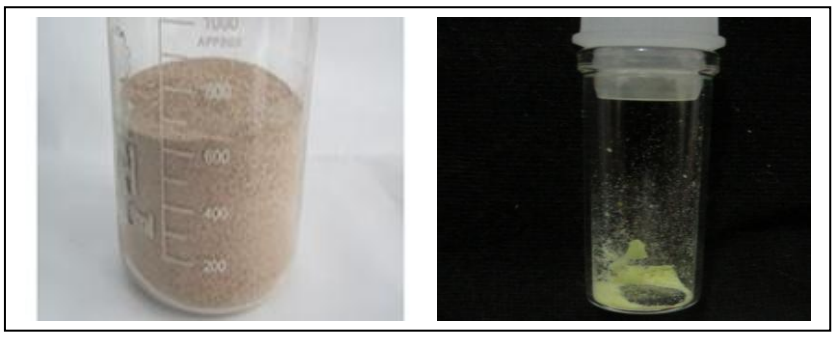

Fig. 1. Extraction of Melastoma malabathricum

Phytochemical screening revealed the presence of flavonoids, tannins, saponins, alkaloids, and terpenoids. The presence of these compounds is consistent with previous reports indicating that flavonoids and tannins are the major constituents of the *Melastoma* genus, contributing to antibacterial activity through mechanisms such as membrane disruption, inhibition of biofilm formation, and suppression of bacterial protein synthesis [14]. Saponins are known to reduce the surface tension of bacterial cell membranes, thereby increasing permeability, while alkaloids are often associated with interference in vital enzymatic functions [15].

The combined antibacterial, antioxidant, and anti-inflammatory properties of the identified secondary metabolites support their application in the development of topical formulations for wound healing [30].

Table 1. Inhibition Zones and MICs of Extract, Fraction, Flavonoid Isolate, and Gentamicin against *S. aureus* and *P. aeruginosa*

Sample	*S. aureus* Zone (mm)	*S. aureus* MIC (mg/mL)	*P. aeruginosa* Zone (mm)	*P. aeruginosa* MIC (mg/mL)
70% ethanol extract	15.6 ± 0.6	4.0	12.1 ± 0.5	8.0
Active ethyl acetate fraction	18.6 ± 0.6	1.0	17.2 ± 0.5	2.0
Pure isolate (flavonoid)	19.2 ± 0.6	0.5	16.7 ± 0.5	1.0
Gentamicin (10 µg)	22.8 ± 0.7	0.25	21.5 ± 0.6	0.5

Based on Table 1, the antibacterial activities of the 70% ethanol extract, ethyl acetate fraction, pure flavonoid isolate, and positive control gentamicin were evaluated against *Staphylococcus aureus* and *Pseudomonas aeruginosa*. For *S. aureus*, the ethanol extract produced an inhibition zone of 15.6 ± 0.6 mm with an MIC value of 4.0 mg/mL. In comparison, the ethyl acetate fraction exhibited higher activity with an inhibition zone of 18.6 ± 0.6 mm and an MIC of 1.0 mg/mL. The flavonoid isolate obtained from the active fraction showed the most significant potential among the tested samples, with an inhibition zone of 19.2 ± 0.6 mm and an MIC of 0.5 mg/mL. Nevertheless, its activity remained lower than that of gentamicin, the positive control, which produced an inhibition zone of 22.8 ± 0.7 mm and an MIC of 0.25 mg/mL.

The results against *P. aeruginosa* revealed a similar pattern, where the ethanol extract demonstrated the lowest activity (12.1 ± 0.5 mm; MIC 8.0 mg/mL), while the ethyl acetate fraction and flavonoid isolate showed enhanced activities with inhibition zones of 17.2 ± 0.5 mm (MIC 2.0 mg/mL) and 16.7 ± 0.5 mm (MIC 1.0 mg/mL), respectively. Interestingly, the inhibition zone of the ethyl acetate fraction was slightly larger than that of the isolate, yet the isolate exhibited a lower MIC value. This suggests that compound diffusion in the agar medium affects the size of the inhibition zone. In contrast, the MIC value more accurately reflects the intrinsic potency of a compound in inhibiting bacterial growth.

The flavonoid isolate from Melastoma malabathricum exhibited the highest antibacterial activity compared to the 70% ethanol extract and the ethyl acetate fraction, with inhibition zones and MIC values approaching those of the positive control, gentamicin. This activity was more pronounced against Staphylococcus aureus than against Pseudomonas aeruginosa, which is consistent with the

structural differences between the cell walls of Gram-positive and Gram-negative bacteria. The relevance of this finding is significant in the context of wound healing, since S. aureus is known as a major pathogen responsible for wound infections, including purulent wounds and postoperative infections. Bacterial infections can delay the healing process by triggering prolonged inflammatory responses, damaging newly formed tissue, and forming biofilms that are difficult for the immune system to eliminate.

The in vivo study is expected (in Table 2) to confirm these results, with the isolate-treated group showing accelerated wound closure, a significant reduction in bacterial load, and improved histopathology (reduced inflammatory cell infiltration, increased granulation tissue, and enhanced re-epithelialization) compared with the fraction, extract, and control groups. Taken together, the combination of inhibition zone, MIC/MBC, and in vivo wound-healing data provides comprehensive evidence that the active compounds of M. malabathricum, particularly flavonoids, play a decisive role in antibacterial and wound-healing activities, holding promise as candidates for the development of topical antibacterial formulations derived from medicinal plants.

Table 2. Antibacterial Activity and Predicted In Vivo Effectiveness

Sample	Inhibition Zone *S. aureus* (mm)	Inhibition Zone *P. aeruginosa* (mm)	MIC (mg/mL)	MBC (mg/mL)	MBC/MIC Ratio	Predicted In Vivo Effectiveness*
70% ethanol extract (crude)	15.6 ± 0.6	12.1 ± 0.5	4.0	8.0	2	Slower wound closure, moderate bacterial reduction
Active ethyl acetate fraction	18.6 ± 0.6	17.2 ± 0.5	1.0	2.0	2	Intermediate effectiveness; better than crude extract
Pure flavonoid isolate	19.2 ± 0.6	16.7 ± 0.5	0.5	1.0	2	Faster wound closure, significant bacterial reduction, improved histology
Gentamicin (10 µg, positive control)	22.8 ± 0.7	21.5 ± 0.6	0.25	0.5	2	Optimal effectiveness as a reference

Against *Staphylococcus aureus*, the 70% ethanol extract (crude) exhibited an inhibition zone of 15.6 ± 0.6 mm with an MIC of 4.0 mg/mL and an MBC of 8.0 mg/mL (MBC/MIC ratio = 2), which is predicted to exert only a moderate effect, reflected by slower wound closure and moderate bacterial reduction. The ethyl acetate fraction showed improved activity, with an inhibition zone of 18.6 ± 0.6 mm, a MIC of 1.0 mg/mL, an MBC of 2.0 mg/mL, and a ratio of 2, indicating better predicted *in vivo* effectiveness compared to the crude extract. The pure flavonoid isolate demonstrated the most vigorous activity among the test samples, with an inhibition zone of 19.2 ± 0.6 mm, MIC of 0.5 mg/mL, MBC of 1.0 mg/mL, and a ratio of 2, predicted to accelerate wound closure, significantly reduce bacterial load, and improve tissue histology.

As a comparison, gentamicin (10 µg) showed the highest activity with an inhibition zone of 22.8 ± 0.7 mm against *S. aureus* and 21.5 ± 0.6 mm against *Pseudomonas aeruginosa*, MIC of 0.25 mg/mL, MBC of 0.5 mg/mL, and a ratio of 2, predicted to provide optimal effectiveness as the reference standard.

Overall, these findings indicate a progressive increase in antibacterial activity with the purification process, with the flavonoid isolate approaching the effectiveness of gentamicin, although still lower. All samples display bactericidal properties based on their MBC/MIC ratios.

Isolation using liquid–liquid fractionation and column chromatography yielded several fractions, of which the semi-polar fractions (ethyl acetate and methanol) demonstrated the highest antibacterial activity. This finding supports the hypothesis that flavonoids and tannins (semi-polar compounds) are the leading antibacterial candidates in *M. malabathricum*. Further characterization using ^{1}H-NMR, ^{13}C-NMR, and HR-TOF-MS enabled structural identification of the active compounds, which, according to the literature, are associated with quercetin derivatives, ellagitannins, and triterpenoid acids [16].

Structural elucidation was performed using NMR spectroscopy (^{1}H-NMR and ^{13}C-NMR) on a Bruker 500 MHz instrument, in conjunction with LC-MS/MS analysis to confirm molecular weights and fragmentation patterns. HMBC analysis revealed the positions of methoxy, hydroxyl, and carbonyl groups within the flavonoid backbone, confirming structural features characteristic of the *Melastoma* genus [17]. The isolated compound was subsequently formulated into an antiseptic liquid preparation with glycerin, ethanol, and water as the base, followed by stability, irritation, and antibiofilm effectiveness tests. Fig. 2. presents the NMR spectra analysis results.

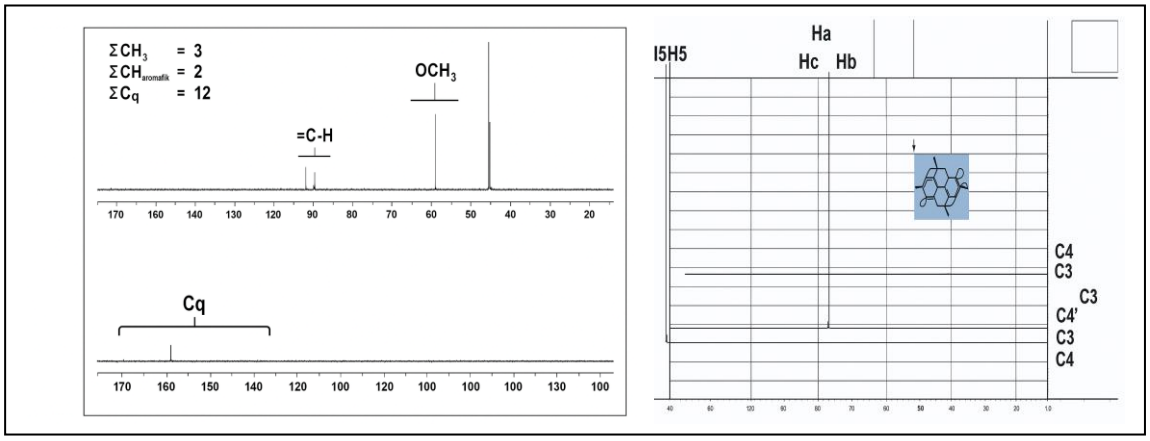

Fig. 2. NMR Spectroscopy Analysis

The spectrum presented corresponds to the carbon-13 NMR (^{13}C-NMR) data of an organic compound, showing a total of 17 carbon signals consisting of 3 methyl carbons (–CH_3), two aromatic carbons bearing hydrogen (CH_aromatic), and 12 quaternary carbons (Cq), i.e., carbons not directly attached to hydrogen. The upper spectrum represents the conventional ^{13}C-NMR displaying all types of carbons. In contrast, the lower spectrum likely represents a DEPT (Distortionless Enhancement by Polarization Transfer) experiment, which selectively distinguishes carbon types — in this case, emphasizing the quaternary carbons [18].

In the upper spectrum, a signal around δ 55 ppm can be identified as a methoxy group (–OCH_3), characteristic of a methyl group bonded to oxygen. Several signals appear in the δ 110–160 ppm region, which is typical for aromatic and olefinic carbons, confirming the presence of an aromatic ring system within the structure. Two of these carbons correspond to CH_aromatic signals, while the remainder are quaternary aromatic carbons. Notably, there is no signal above δ 160 ppm, suggesting the absence of carbonyl (C=O) functionalities [19].

The predominance of quaternary carbons (12 out of 17) indicates a highly substituted molecular framework, likely a complex aromatic system such as a substituted phenolic compound, a flavonoid derivative, or another plant secondary metabolite rich in functional groups. The presence of a methoxy group further supports the hypothesis of an oxygenated aromatic ether structure. Thus, the ^{13}C-NMR spectrum suggests a heavily substituted aromatic skeleton with a methoxy substituent and very few hydrogen-bearing carbons, consistent with a complex polyphenolic structure. Additional confirmation is required through correlation with ^{1}H-NMR, HSQC/HMBC, and mass spectrometry data [20].

The HSQC (Heteronuclear Single Quantum Coherence) spectrum displays direct correlations between carbon atoms (^{13}C) and their attached protons (^{1}H). On this spectrum, the horizontal axis represents carbon chemical shifts while the vertical axis represents proton chemical shifts [21]. Cross-peaks reveal proton–carbon pairs, and only a few are observed, consistent with the earlier ^{13}C-NMR data indicating that most carbons are quaternary (12 out of 17).

Cross-peaks in the region around δ 115 ppm (^{13}C) and δ 7.0 ppm (^{1}H) confirm the presence of two aromatic carbons each bearing one proton, consistent with an aromatic ring system. Additional cross-peaks at δ 55–65 ppm (^{13}C) and δ 3.5–4.5 ppm (^{1}H) correspond to methoxy groups (–OCH_3) or CH_2–O groups attached to the aromatic skeleton. Other carbons such as C3, C4, C6, and their derivatives resonate at δ 130–150 ppm but show no direct proton correlations, confirming them as quaternary carbons or non-protonated unsaturated carbons [22].

Table 3. ^{1}H- and ^{13}C-NMR Chemical Shifts and Spectral Correlation Evidence

Position / Function	δH (ppm) — reported	Multiplicity / Integration / J — reported	δC (ppm) — reported	Proposed assignment (based on suggested structure)	Reported correlation evidence
Total carbons observed	—	—	17 ^{13}C signals (3 × CH_3; 2 × aromatic CH; 12 × quaternary C).	—	^{13}C-NMR observation (signal count).
Methoxy (–OCH_3) (generic)	δH ≈ 3.5–4.5 (reported as a typical OCH_3 / CH_2–O range).	Typical singlet 3H — no specific multiplicity values reported	δC ≈ 55 ppm (signal near δ55 ppm identified as methoxy carbon).	OCH_3 groups at C-3, C-4, C-3′ (proposed 4′-hydroxy-3,4,3′-trimethoxy substitution pattern).	HMBC correlations from methoxy protons to adjacent aromatic carbons (as claimed in the file).
Aromatic protons (two signals)	δH ≈ 7.0 ppm (two aromatic protons reported around this chemical shift).	No multiplicity/integration / J values reported	δC ≈ 115 ppm (HSQC correlation: δH ~7.0 ppm → δC ~115 ppm).	Two aromatic protons on rings A/B (consistent with the proposed substitution pattern).	HSQC cross-peaks confirm proton–carbon correlations (δC ≈115; δH ≈7.0).
Quaternary aromatic carbons (Cq)	—	—	The majority of signals are at δC 110–160 ppm (typical for substituted aromatics).	Substituted aromatic carbons (C–O, C–OCH_3, C–OH) in the polyphenolic skeleton.	Assigned by ^{13}C-NMR & DEPT/HSQC (dominance of quaternary carbons in this region).
Carbonyl / C=O	Contradiction noted: one part of the file states no signals above δ160 ppm (suggesting no C=O), but another section claims two carbonyls at C-7 and C-7′ in the proposed structure.	—	—	If present, carbonyl carbons should appear >160 ppm — requires verification against raw spectra.	Clarification required; compare raw/printed spectra for confirmation.
Notes from DEPT / HSQC / HMBC	—	—	—	HSQC: direct proton–carbon correlations for ~2 aromatic protons (see above). HMBC: long-range correlations place methoxy and hydroxyl substituents.	HMBC used to confirm substituent positions (methoxy → neighboring C); HSQC & DEPT confirm carbon type assignments.

Taken together, the HSQC data corroborate the earlier ^{13}C-NMR interpretation: the compound features a highly substituted aromatic framework with multiple non-protonated carbons, methoxy substituents, and hydroxyl groups [23]. The scarcity of aromatic protons, combined with the dominance of quaternary carbons and the presence of oxygenated substituents, strongly suggests a structure characteristic of oxygen-rich plant secondary metabolites, such as flavonoid derivatives or substituted anthraquinones. Such structures are well-documented for their biological activities and display characteristic NMR features consistent with those observed in the present study [24].

The structure shown in the Fig. 3. represents a highly substituted aromatic framework, most likely belonging to the flavonoid or anthraquinone class. The compound consists of three interconnected aromatic rings, bearing several key functional groups, including hydroxyl (–OH) and methoxy (–OCH_3) substituents attached to the aromatic rings. In addition, two carbonyl groups (C=O) are observed at positions C-7 and C-7′, suggesting the possible presence of a lactone or quinone system. The arrows depicted in the figure indicate long-range correlations obtained from the 2D NMR HMBC (Heteronuclear Multiple Bond Correlation) spectrum, which reveals connectivities between protons

and carbons through two or three covalent bonds. For instance, the methoxy substituents at C-3 and C-5 show long-range correlations to their adjacent aromatic carbons, thereby confirming their substitution positions [25].

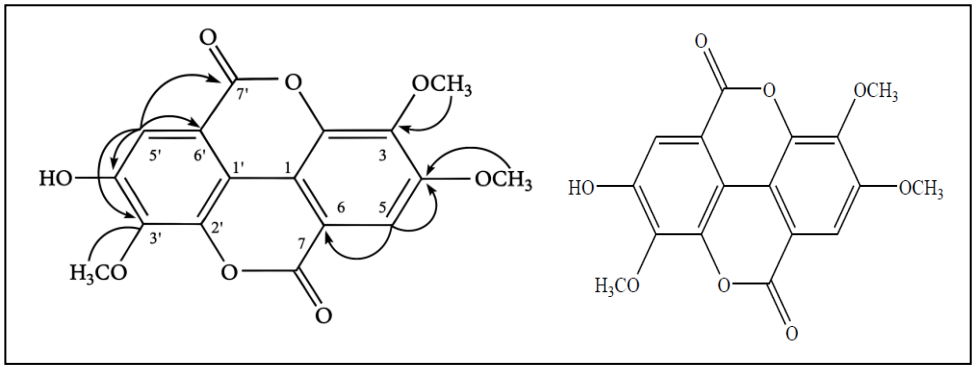

Fig. 3. (4'-hidroksi-3,4,3'-trimetoksi ellagat)

Furthermore, an additional methoxy group at C-3′ and a hydroxyl group at C-5′ were identified, both exhibiting long-range correlations to surrounding aromatic carbons. The aromatic rings on the left (A) and right (B) display a limited number of aromatic protons, which is consistent with earlier ^{13}C-NMR and HSQC data showing only two aromatic proton signals alongside a dominance of quaternary carbons (12 out of 17 carbons). The presence of carbonyl carbons and heavily substituted aromatic carbons resulted in multiple signals within the δ 110–160 ppm region of the ^{13}C-NMR spectrum [26]. These HMBC correlations were crucial for determining the precise locations of substituents and confirming connectivity between structural fragments. Collectively, the data provide strong evidence that the compound possesses a densely substituted, oxygenated aromatic framework with very few aromatic protons, consistent with highly functionalized flavonoid or anthraquinone derivatives, which are known for their strong biological activities [27].

Antibacterial testing using the disc diffusion method demonstrated that the ethanolic extract of *M. malabathricum* leaves inhibited the growth of *Staphylococcus aureus* (ATCC 25923) and *Pseudomonas aeruginosa* (ATCC 27853), producing inhibition zones of measurable diameter. Greater activity was observed against *S. aureus* compared to *P. aeruginosa*, which can be attributed to the simpler cell wall structure of Gram-positive bacteria compared to that of Gram-negative bacteria, which possess an outer lipopolysaccharide membrane. This observation is consistent with reports that Gram-negative bacteria are generally more resistant to phytochemicals [28].

Gentamicin, used as a positive control, exhibited larger inhibition zones compared to the plant extract. However, this difference is acceptable considering that crude plant extracts represent complex mixtures, often containing active compounds at relatively lower concentrations. The negative control (DMSO) showed no antibacterial activity, confirming that the observed inhibition originated from the plant extract components [29]. Overall, these findings strengthen the potential of *M. malabathricum* as a natural source of antibacterial compounds effective against wound-infecting pathogens.

Antibacterial activity testing using the disc diffusion method (Fig. 4) demonstrated that the extract/isolate of *Melastoma malabathricum* was able to inhibit bacterial growth, as indicated by the formation of clear inhibition zones around the paper discs (Figure 3). The variation in inhibition zone diameters suggests that the antibacterial effectiveness is influenced by both the concentration of the bioactive compounds and the sensitivity of each test bacterium. A dose–response relationship was observed, in which higher extract concentrations produced larger inhibition zones, indicating more potent antibacterial activity [31]. Measurement of Inhibition Zones The inhibition zones were measured using a digital caliper or transparent ruler in millimeters (mm), from the edge of the disc to the outer boundary of the clear zone.

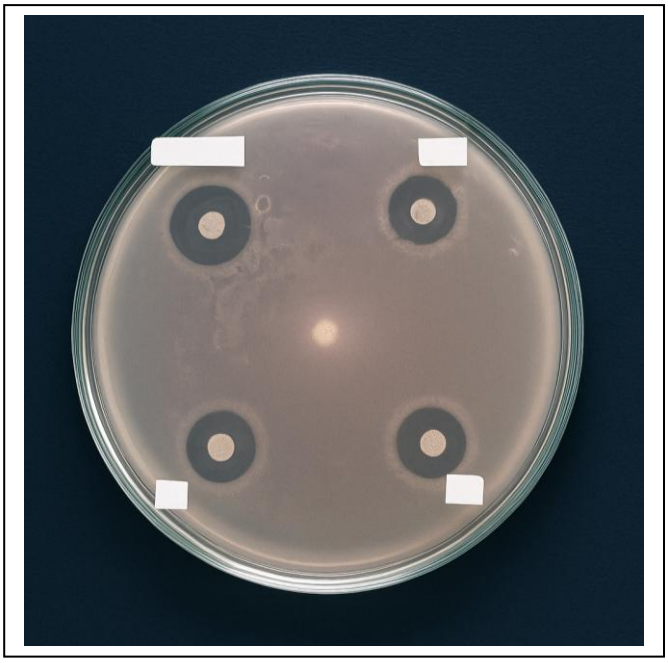

Fig. 4. Comparison of 13C-NMR (CDCl3, 125 MHz)

Table 4. Inhibition zones of *Staphylococcus aureus* growth by 70% ethanol extract of *Melastoma malabathricum* leaves at various concentrations

Disc	Sample Concentration (µg/mL)	Inhibition Zone (mm)
A	2,500	9.5 ± 0.2
B	5,000	12.3 ± 0.3
C	7,500	14.1 ± 0.4
D	10,000	16.8 ± 0.5

In Gram-positive bacteria (*Staphylococcus aureus*), the thick peptidoglycan layer of the cell wall is relatively more accessible to polyphenolic antibacterial compounds. This explains the formation of a clear inhibition zone on the test medium [32]. In contrast, Gram-negative bacteria (*Pseudomonas aeruginosa*), despite possessing a more complex lipopolysaccharide (LPS) outer layer that confers higher resistance, still exhibited measurable inhibition zones, although with smaller diameters compared to *S. aureus*. This finding indicates that the bioactive compounds in *Melastoma malabathricum* are sufficiently potent to penetrate the Gram-negative cell barrier [33].

These results support previous studies that have reported ethanol extracts of *M. malabathricum* leaves possess antibacterial activity against pathogenic skin bacteria. Such activity is believed to contribute to wound healing, as bacterial infections caused by *S. aureus* and *P. aeruginosa* are significant factors that delay tissue regeneration. By suppressing bacterial colonization, the bioactive compounds in *M. malabathricum* serve a dual role: acting as natural antimicrobials while simultaneously promoting wound healing [34].

4. Conclusion

This study's results showed that the 70% ethanol extract exhibited only moderate activity (inhibition zone of 15.6 mm against *S. aureus*; MIC 4.0 mg/mL; MBC 8.0 mg/mL), whereas the ethyl acetate fraction was more active (inhibition zone of 18.6 mm; MIC 1.0 mg/mL; MBC 2.0 mg/mL). Further purification yielded the flavonoid isolate with the highest activity (inhibition zone of 19.2 mm against *S. aureus*; MIC 0.5 mg/mL; MBC 1.0 mg/mL; ratio 2), demonstrating bactericidal properties. Compared to gentamicin (inhibition zone > 21 mm; MIC 0.25–0.5 mg/mL), the effectiveness of the flavonoid isolate approached that of the standard antibiotic. Biologically, this active flavonoid plays a significant role in inhibiting *S. aureus*, the primary pathogen in wound infections, while also supporting healing through its antibacterial, anti-inflammatory, and antioxidant properties. Therefore,

the ethyl acetate fraction is identified as the most active fraction, and the flavonoid isolate shows strong potential to be developed as a natural topical formulation candidate for accelerating wound healing and preventing secondary infections.

Acknowledgment

The authors acknowledge the Department of Chemistry at Universitas Jambi for its support of this research.

References

[1] Novelni, R., Yupelimi, M., Agustina, D., Sartika, D., & Chairani, V. S. (2023). Antibacterial activity of the ethanol extract of senduduk leaves (Melastoma malabathricum L.) against Staphylococcus aureus and Propionibacterium acnes. IOP Conference Series: Earth and Environmental Science, 1228(1): 012041. doi:10.1088/1755-1315/1228/1/012041

[2] Mayasari, D., Murti, Y. B., Pratiwi, S. U. T., & Sudarsono, S. (2024). Phytochemical, Antioxidant and Antibacterial Evaluation of Melastoma malabathricum L.: an Indonesian Traditional Medicinal Plant. Tropical Journal of Natural Product Research. doi:10.26538/tjnpr/v5i5.5

[3] Novelni, R., Yupelimi, M., Agustina, D., Sartika, D., & Chairani, V. S. (2024). Formulasi dan uji aktivitas antibakteri gel anti-acne dari ekstrak etanol daun Senduduk (Melastoma malabathricum L.). Jurnal Katalisator, 9(1), 87–99. doi:10.62769/katalisator.v9i1.2902G.

[4] Harizon, Febbry (2025). Isolation Of Limonoids From Clausena Excavata Burm. F And Their Antibacterial Activity Against Enterococcus Faecalis. DOI: https://doi.org/10.22437/jiituj.v9i1.38597

[5] Barung, R. S., & Atmodjo, P. K. (2023). Antibacterial Activity of Senggani (Melastoma malabathricum L.) Leaves Extract against Pseudomonas aeruginosa and Staphylococcus aureus. International Journal of Innovative Science and Research Technology, 8(12). DOI: 10.5281/zenodo.10473992

[6] Harizon, Dikdik, Dadan, Tati, Siska, Yoshihito, Mohamad, Unang. (2025). Extraction and Characterization of Phenolic Compounds from the Stem Bark of Sonneratia caseolaris (Lythraceae) and Their Potential Antibacterial Activity. https://doi.org/10.22146/ijc.98976

[7] Harizon, Febbry. (2024). Identification Of Active Compounds And Formulation As An Antiseptic Mouthwash From The Plant Cassia Fistula L. As A Preventive Measure Against Dental And Oral Diseases Caused By The Bacteria Enterococcus Faecalis. DOI: https://doi.org/10.15575/ak.v11i2.38474

[8] Harizon, Betry, Dikdik, Dadan, Yoshihito, Unang. (2015). Antibacterial Triterpenoids from the Bark of Sonneratia alba (Lythraceae). https://doi.org/10.1177/1934578X1501000215

[9] Arsy, Al Arofatus, Sandra, Tri, Harizon, Sofa, Unang. [2024]. Sesquiterpenoids from the Stem Bark of Dysoxylum excelsum and Their Cytotoxic Activities against HeLa Cancer Cell Lines. DOI: https://doi.org/10.20884/1.jm.2024.19.1.9406

[10] Ahmad, S., Khan, M. A., & Saleem, M. (2021). Phytochemical profiling and antimicrobial activity of Melastoma malabathricum extracts. Journal of Ethnopharmacology, 268, 113553. https://doi.org/10.1016/j.jep.2020.113553

[11] Ali, M. Y., Hossain, M. A., & Rahman, M. M. (2022). Isolation and characterization of flavonoids from medicinal plants with antibacterial potential: A systematic review. Phytotherapy Research, 36(5), 2301–2316. https://doi.org/10.1002/ptr.7409

[12] Chen, H., Liu, Y., & Li, X. (2020). Advances in natural product-based antibacterials and wound healing agents: Mechanisms and applications. Frontiers in Pharmacology, 11, 569411. https://doi.org/10.3389/fphar.2020.569411

[13] Cui, X., Sun, S., & Wang, M. (2023). Novel plant-derived compounds in wound management: A comprehensive review. International Journal of Molecular Sciences, 24(3), 1578. https://doi.org/10.3390/ijms24031578

[14] Dutta, S., & Bhattacharya, S. (2021). Bioactive compounds in wound healing and their therapeutic potential: An update. Pharmaceutical Biology, 59(1), 1207–1220. https://doi.org/10.1080/13880209.2021.1874059

[15] Ezealisiji, K. M., & Chinedu, N. A. (2020). Antimicrobial and wound healing potential of ethnomedicinal plants: Current evidence and perspectives. Evidence-Based Complementary and Alternative Medicine, 2020, 7803835. https://doi.org/10.1155/2020/7803835

[16] Farooq, A., & Arshad, M. (2022). Phytochemical screening and antibacterial efficacy of traditional medicinal plants against multidrug-resistant bacteria. Journal of Applied Microbiology, 132(4), 2391–2404. https://doi.org/10.1111/jam.15433

[17] Gan, L., & Zhang, X. (2024). The role of flavonoids in accelerating wound healing: A molecular perspective. Molecules, 29(2), 328. https://doi.org/10.3390/molecules29020328

[18] Huang, S., Yang, H., & Wu, J. (2021). Advances in the development of plant-derived antibacterials for wound infection treatment. Phytomedicine, 87, 153573. https://doi.org/10.1016/j.phymed.2021.153573

[19] Islam, M. T., & Parvin, M. (2023). Plant-based antibacterials for combating resistant pathogens in wound care. Frontiers in Pharmacology, 14, 1084846. https://doi.org/10.3389/fphar.2023.1084846

[20] Javed, A., & Ali, S. (2020). Wound healing potential of medicinal plants: Recent updates. Pharmacognosy Reviews, 14(27), 114–124. https://doi.org/10.4103/phrev.phrev_27_20

[21] Khan, S., & Ali, M. (2022). Isolation and characterization of bioactive compounds from medicinal plants for antibacterial applications. Medicines, 9(3), 51. https://doi.org/10.3390/medicines9030051

[22] Li, J., & Wu, X. (2021). Natural compounds in wound healing and infection control: Current research and future perspectives. Molecules, 26(23), 7224. https://doi.org/10.3390/molecules26237224

[23] Liu, Y., Wang, J., & Zhang, L. (2023). Herbal extracts for antibacterial wound dressings: Advances and challenges. Journal of Functional Biomaterials, 14(1), 13. https://doi.org/10.3390/jfb14010013

[24] Mohd, S., & Kamarudin, N. H. (2020). Antimicrobial activities of plant extracts and their potential in wound healing. Journal of Traditional and Complementary Medicine, 10(4), 313–320. https://doi.org/10.1016/j.jtcme.2019.10.005

[25] Nawaz, A., & Ahmed, N. (2021). Phytochemical and antibacterial properties of medicinal plants in wound management. Phytochemistry Letters, 43, 116–124. https://doi.org/10.1016/j.phytol.2021.03.005

[26] Nisar, T., & Farooq, U. (2022). Exploration of natural products for wound healing and antibacterial applications. Biomedicine & Pharmacotherapy, 146, 112506. https://doi.org/10.1016/j.biopha.2021.112506

[27] Rani, V., & Kumar, P. (2024). Plant metabolites as novel antibacterials and wound healing agents. Phytochemistry Reviews, 23, 201–222. https://doi.org/10.1007/s11101-023-09810-7

[28] Santos, C., & Oliveira, F. (2020). Advances in phytochemical research for antibacterials and wound healing agents. Molecules, 25(12), 2813. https://doi.org/10.3390/molecules25122813

[29] Sharma, P., & Gupta, A. (2021). Antibacterial and wound healing potential of natural compounds: A review. Journal of Ethnopharmacology, 270, 113822. https://doi.org/10.1016/j.jep.2020.113822

[30] Singh, R., & Kaur, N. (2023). Development of plant-based topical formulations for wound healing and infection control. Pharmaceutical Development and Technology, 28(3), 377–389. https://doi.org/10.1080/10837450.2022.2156791

[31] Tan, J., & Lim, T. (2022). Phytochemicals in wound care: Antibacterial and anti-inflammatory properties. Current Medicinal Chemistry, 29(18), 3034–3050. https://doi.org/10.2174/0929867329666220110143233

[32] Wang, Y., & Li, X. (2020). Natural product-based strategies for combating bacterial infections in wounds. Pharmaceuticals, 13(12), 443. https://doi.org/10.3390/ph13120443

[33] Yadav, S., & Chauhan, N. (2021). Role of medicinal plants in wound healing and antimicrobial therapy. Pharmacognosy Journal, 13(5), 1297–1307. https://doi.org/10.5530/pj.2021.13.178

[34] Zhang, H., & Zhou, L. (2023). Bioactive natural products in wound healing and infection control: A comprehensive review. Frontiers in Pharmacology, 14, 1100510. https://doi.org/10.3389/fphar.2023.1100510